International Journal of Mass Spectrometry and Ion Physics, 40 (1981) 185—193
Elsevier Scientific Publishing Company, Amsterdam — Printed in The Netherlands

A TIME-OF-FLIGHT MASS SPECTROMETER FOR MEASUREMENT OF SECONDARY ION MASS SPECTRA

B.T. CHAIT * and K.G. STANDING

Physics Department, University of Manitoba, Winnipeg, Manitoba R3T 2N2 (Canada)

(Received 25 March 1981)

ABSTRACT

A time-of-flight mass spectrometer has been constructed at the University of Manitoba. In this instrument, bursts of alkali-metal ions of ~10 ns duration strike a thin layer of organic material deposited onto a metal backing. The secondary ions produced are accelerated across a fixed potential ⩽10 kV, then travel down a flight tube 1.6 m long. Measurement of the time of flight determines the mass-to-charge ratio of the ions.

Mass spectra from biomolecules with masses up to 1355 u have been measured with the instrument. They exhibit significant quasimolecular ion peaks.

INTRODUCTION

For some time there has been growing interest in the measurement of the masses of large biomolecules. Since most of these molecules are involatile and fragile, they are difficult to study by conventional mass spectrometry. However, in recent years several so-called "soft-ionization" techniques have been developed [1]; these allow large biomolecules to be observed as molecular or quasimolecular ions.

In one such method, a primary ion desorbs and ionizes the molecule from a thin layer of the compound on a metallic surface. Macfarlane and Torgerson [2] first demonstrated this technique with fission fragments from ^{252}Cf, using a time-of-flight mass spectrometer [3]. Later, Benninghoven and Sichtermann obtained somewhat similar results with 2-keV argon ions [4], and Dück et al. used 8—40-MeV accelerated ions (^{16}O and ^{32}S) for the same purpose [5].

A review by Macfarlane [6] describes progress in this field using fission fragments. Results obtained with low-energy ions have been given in several recent papers [7—9]. All measurements with fission fragments and high-energy accelerated ions have been made by time-of-flight methods. On the

* Now at The Rockefeller University, New York, NY 10021, U.S.A.

0020-7381/81/0000—0000/$02.50

other hand, all previous measurements with low-energy ions have been made with magnetic or quadrupole spectrometers.

We here report the construction of a time-of-flight mass spectrometer for measurement of secondary ion mass spectra produced by low-energy primary ions.

THE MASS SPECTROMETER

The instrument is similar to the mass spectrometer of Macfarlane and Torgerson [3], but with the addition of a pulsed ion source. The principle of the device is illustrated in Fig. 1. Here a thin layer of organic material deposited onto the target backing is struck by a succession of ion pulses from the source. When these pulses of primary ions hit the target, they may liberate secondary ions. Each secondary ion (charge q_s, mass m_s) is accelerated to an energy $q_s V_s$ by the electric field between the target and a coplanar grid. Since $q_s V_s = 1/2\ m_s v_s^2$, the ion continues down the flight tube with a velocity $v_s = [2q_s V_s/m_s]^{1/2}$. The time of flight of the ion determines its velocity v_s and hence its ratio of mass to charge.

The spacing between the target and the grid (60% transmission) is 2 mm. The target has been operated at potentials V_s up to 10 kV. Thus at $V_s = 10$ kV, an ion with $m_s/z \simeq 190$ requires 40 ns to reach its full velocity $v_s = 10^7$ cm s^{-1} as it passes through the grid into the field-free flight tube. For $m_s/z \simeq 1200$, the corresponding figures are 100 ns and 4×10^6 cm s^{-1}.

The system is almost entirely metal-sealed. Sublimation pumps and ion pumps are used to provide operating pressures in the 10^{-8} torr range. Rough pumping is done by sorption pumps and a venturi pump so that clean vacuum conditions are maintained throughout evacuation. The apparatus is constructed of non-magnetic stainless steel. The flight tube has a length of ~1.6 m and an internal diameter of ~15 cm.

A vacuum lock is provided on a side tube, so that targets may be changed without disturbing the vacuum in the main system. Five targets are mounted in line on a ceramic sample-holder which can be moved by a rack-and-pinion mechanism. The target backings are prepared by stretching 6.4-μm aluminized polyester film over a stainless-steel ring (1.8 cm o.d.) by means of a snugly

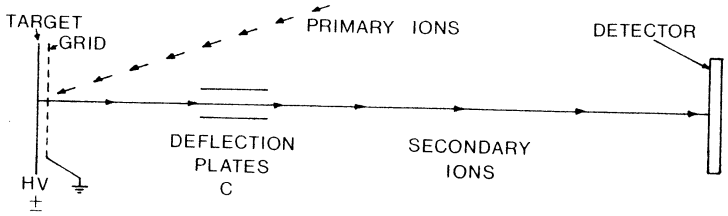

Fig. 1. Schematic diagram of the time-of-flight mass spectrometer (not to scale).

fitted outer ring. This provides a surface which is accurately plane. The sample is then electrosprayed from solution [10] onto the aluminized side of the target backing to give a sample thickness of ~10 $\mu g\ cm^{-2}$.

THE ION SOURCE

Figure 2 shows the pulsed-ion gun. Alkali-metal ions (Li^+, Na^+, K^+, or Cs^+) are emitted thermionically from a small glassy bead of alkali aluminosilicate [11,12] melted onto the end of a tungsten hairpin filament. This type of source was chosen because of its simplicity, low cost, and minimal pumping requirements.

The electrostatic design of the source is based on the three-electrode guns widely used in electron microscopy [13,14]. The plane cathode is operated at ground potential. The position of its aperture (1.5 mm diameter) may be adjusted externally in the plane perpendicular to the ion beam axis, in order to provide accurate alignment of the extracted beam. The filament is held at a potential V_p, so the energy of a primary ion (mass m_p, charge q_p) leaving the source is $q_p V_p$. The anode shield is set at a potential ($V_p \pm$ a few volts) adjusted to give an optimum beam.

The beam is focused by a gridded Einzel lens [15] to a spot of ~100 μm diameter in the plane containing the defining slit. It is swept rapidly across the 100-μm-wide slit by a voltage pulse V_{def} applied to the deflection plates "A" (see Fig. 2). The resulting short bursts of ions pass through the secondary ion accelerating grid and arrive at the target surface with an ion energy $q_p(V_p - V_s)$. (A second ion burst would normally appear on the falling edge of the voltage pulse, but this is removed by applying a delayed voltage pulse to the other set of deflection plates "B" oriented at right angles to the first set). For a beam focused to a point, the duration of the ion burst passing through the slit is proportional to $(m_p V_p)^{1/2}/V_{def}$; more general cases are treated by Fowler and Good [16].

The ion source has been operated thus far at potentials V_p up to 25 kV, corresponding to an initial energy of 25 keV. The duration of the ion burst passing through the slit has varied from ~6 to ~50 ns, depending on the

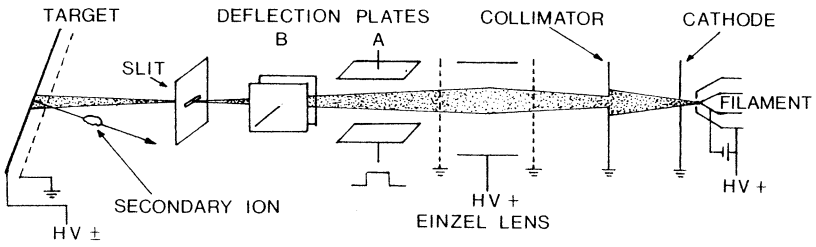

Fig. 2. Pulsed positive-ion source.

energy and the ion species. Its shortness has been limited primarily by the small deflection voltage (V_{def} = 50 V) provided by our present pulser *. For a given pulse duration, the ion flux at the target may be set to a suitable value by varying the d.c. ion-beam current; this is done by adjustment of the filament current. Under various operating conditions, the d.c. current at the plane of the slit has ranged from 0.3 to 30 nA. Normally the beam is adjusted so that ~100 to ~1000 ions per pulse pass through the slit and hit the target at a repetition frequency of 5—10 kHz, corresponding to an *average* ion current of ~0.1 to ~1 pA. Since the target beam spot has a diameter of ~2 mm, the average ion current density on the beam spot is ~3 to ~30 pA cm^{-2}, several orders of magnitude smaller than current densities typically used with magnetic and quadrupole instruments [7—9].

The primary ion beam strikes the target at an angle of incidence of ~20°. Either positive or negative secondary ions may be observed by reversing the potential applied to the target. When a positive potential $V_s = |V|$ is applied to the target to accelerate positive secondary ions, the positively charged primary ions are decelerated in the region between the grid and the target. Their energy at the target is $q_p(V_p - V_s) = q_p V_p - q_p|V|$, i.e., the initial energy minus $q_p|V|$. The filament potential V_p must be $\geqslant |V|$, and primary energies are available from the limit set by the maximum value of V_p, down to zero. Conversely, when a negative potential $V_s = -|V|$ is applied to the target to accelerate negative secondary ions, the primary ions are given an additional energy $q_p|V|$ as they are accelerated from the grid to the target. Thus for negative secondary ions, incident primary beam energies less than $q_p|V|$ are not accessible, and the primary beam energy at the target is $q_p(V_p + |V|) = q_p V_p + q_p|V|$, i.e., the initial energy plus $q_p|V|$.

ION DETECTION AND MEASUREMENT

The ions are detected by a chevron microchannel electron multiplier at the end of the flight tube. Time of flight is measured by conventional nuclear timing circuits, as shown in Fig. 3. Amplified pulses from the electron multiplier trigger a discriminator, which supplies the "stop" signal for a time-to-pulse-height converter (TAC). The "start" signal for the TAC is provided by a precision time-mark generator, which also triggers the pulser which delivers the deflection pulse V_{def} for the primary ion beam. Thus the TAC start is synchronized with the arrival of the primary ion burst at the target, and the TAC stops when a secondary ion arrives at the detector. The TAC output, proportional to this time interval, is connected to an analogue-to-digital converter (ADC), whose output is recorded and displayed by a pulse-height analyzer. When examining a complete mass spectrum, we have used typically 4000 channels of ~10 ns/channel, or a total timing period of ~40 μs.

* The apparatus is specified in detail in Fig. 3.

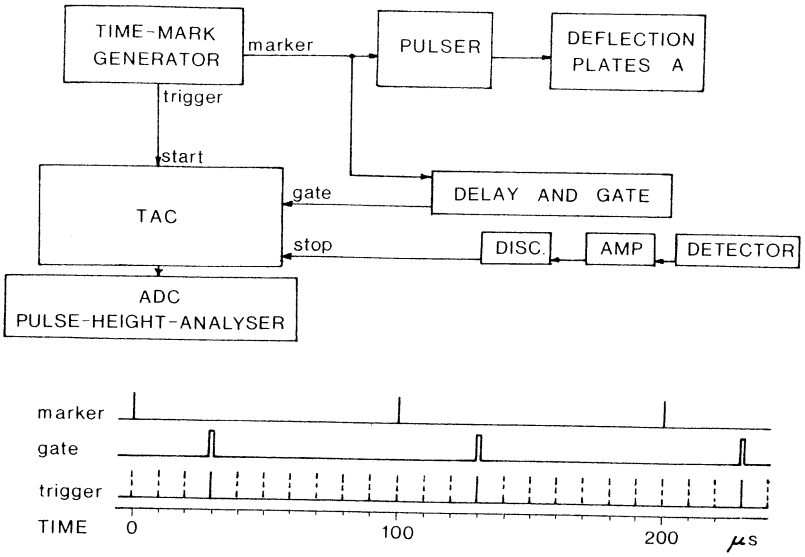

Fig. 3. Schematic diagram of the timing circuits. The example above shows the timing sequence for primary pulses separated by 100 μs and the TAC start delayed by 30 μs. The ungated trigger pulses are shown as dashed lines; pulses separated by 10 μs are shown for clarity, although the normal separation used was 1 μs.

The apparatus was as follows: Tektronix 184 Time-Mark Generator (Tektronix Inc., Portland, OR, U.S.A.); E-H 131 Pulse Generator (E-H Research Laboratories, Oakland, CA, U.S.A.); Ortec 416 A Gate and Delay Generators; Ortec 442 Linear Gate and Stretcher; Ortec 467 Time-to-Pulse-Height Converter; Ortec Discriminator 463; Ortec Preamplifier 142B (Ortec Inc., Oak Ridge, TN, U.S.A.); Inotech Pulse-Height Analyzer Ultima/2, IT 3408 (Norland Corp., Fort Atkinson, WI, U.S.A.); Varian Microchannel Plates 8900 ZS (Varian LSE Division, Palo Alto, CA, U.S.A.).

At high counting rates several ions may arrive at the detector in a given timing period, but the system is capable of measuring only one. When more than one particle is detected in a given period, only the earliest one (the one of lowest mass) will be registered. This can produce significant distortion of the spectrum, particularly for large biomolecules, where the quasimolecular ions may be several orders of magnitude less intense than the fragments. (A direct time-to-digital converter [3,17] is largely free of such distortion, since it can record a number of events per sweep.) In our case, the effect is reduced by running at TAC counting rates $\leqslant 10\%$ of the pulser rate. When the whole spectrum is being examined, the ion beam current is reduced to a value which gives a counting rate within this limit. The loss of counts for ions of high mass is then $\leqslant 10\%$ provided that there is no correlation between the production of such ions and of fragments of lower mass. Correlations have been reported, however [18], so the results must be interpreted with caution. When examining high-mass ions it is usually more satisfactory to reduce

the counting rate by delaying the TAC start, as described below. Only heavy ions — i.e. those arriving after the TAC start — are then recorded, and the abundant low-mass ions do not contribute to the distortion.

In its simplest form, the system has reduced accuracy for long conversion times, because of the non-linearity and jitter present in the analogue TAC and ADC circuits. (A direct time-to-digital converter is almost free of this difficulty.) For example, minimum specifications for the TAC used here (see Fig. 3) require a time resolution of 0.01% of full range, integral nonlinearity of 0.1% of full range, and a temperature stability of 0.015%/°C. Thus for a 40-μs timing period a time resolution no better than ~4 ns and nonlinearities of ~40 ns may be expected. The errors may, however, be largely eliminated by delaying the TAC start signal by a fixed amount, which is conveniently done here by use of the time-mark generator. This unit has two synchronized outputs ("marker" and "trigger") whose periods may be set independently as multiples of the period of the reference oscillator (0.1 μs). In our application, shown schematically in Fig. 3, the "marker" output triggers the pulser which deflects the primary ions; it therefore determines the time at which the secondary ions leave the target. After passing through a variable delay the "marker" pulse also generates a gate signal ~0.3 μs wide which is applied to the TAC "gate" input. The "trigger" output from the time-mark generator is applied to the TAC "start", but it is only effective when coincident with the gate signal. Thus the start may be delayed by any multiple of the "trigger" period. A typical case is shown in Fig. 3. Since the error in "trigger" timing is determined by the stability of the 10-MHz reference oscillator (0.0003% in 24 h), a long time of flight may be measured with an accuracy corresponding to a much shorter time interval.

The linearity of a given timing period is calibrated in a similar way, but with the "marker" output feeding the TAC "start", and the "trigger" output feeding the TAC "stop". As the gating signal delay is changed, calibration peaks are recorded over the whole time spectrum; 1-μs intervals have normally been adequate. Channel numbers on the pulse-height analyzer may then be converted to corrected times t_c by interpolation between the calibration peaks. The ion mass-to-charge ratio is calculated from the equation $\sqrt{m_s/z} = a + bt_c$, where the constants a and b are determined from two peaks corresponding to known masses.

A check on the calibration is provided by a direct comparison of the position of a given peak with one of lower mass. For this comparison, the accelerating voltage is reduced until the time of flight of the lighter ion is the same as the previous time of flight of the heavier one. The ratio of the masses is then just the ratio of the voltages, which may be measured with high accuracy.

PERFORMANCE

Mass spectra of a number of fragile and involatile molecules have been obtained with the instrument for masses up to 1355 u. Typical examples are

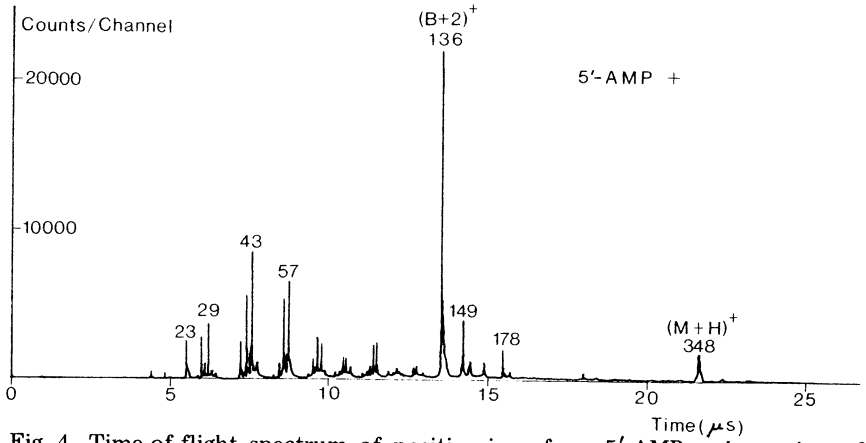

Fig. 4. Time-of-flight spectrum of positive ions from 5′-AMP: primary ions, 8-keV Cs^+; secondary ion energy, 10 keV.

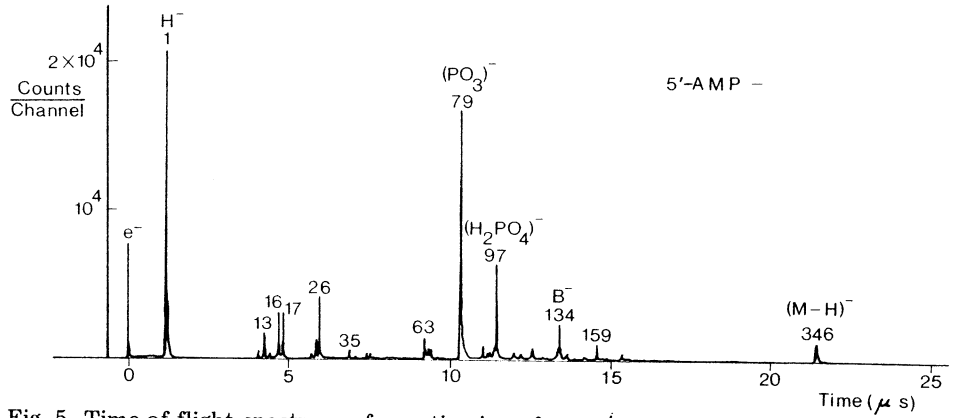

Fig. 5. Time-of-flight spectrum of negative ions from 5′-AMP: primary ions, 15-keV Cs^+; secondary ion energy, 10 keV.

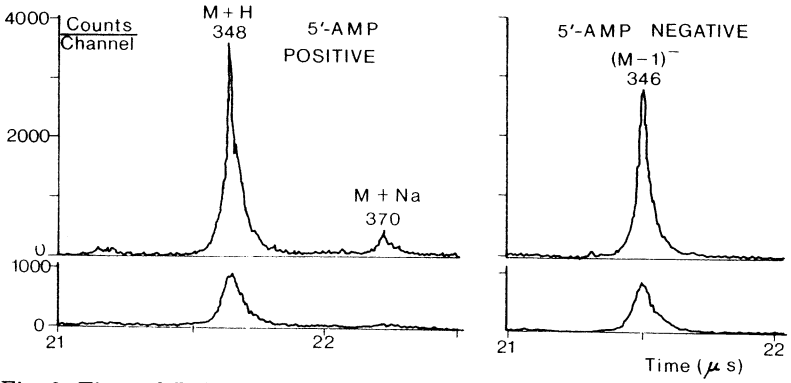

Fig. 6. Time-of-flight spectra of positive and negative ions from 5′-AMP: ion energies as in Figs. 4 and 5. The upper spectra are the normal ones; the lower spectra are taken with 1000 V applied across the deflecting plates "C" of Fig. 1.

shown in Figs. 4—6, the positive and negative time-of-flight spectra of the nucleotide adenosine 5′-monophosphate (5′-AMP). Quasimolecular ions corresponding to M + H, M + Na, and M — H are prominent in Figs. 4 and 5, as are ions corresponding to the adenosine base B.

Figure 6 shows the positive and negative spectra near the quasimolecular peaks on an expanded scale. Here the upper curves are the normal spectra, while the lower ones are the spectra obtained when charged particles are deflected out of the counter by applying a voltage of 1000 V across the secondary ion deflection plates "C" shown in Fig. 1; these plates are ~50 cm downstream of the target. The counts observed then presumably arise from neutral fragments produced by disintegration of ions in the first 50 cm (~10 μs) of flight. Clearly a substantial proportion of the M + H and M — H ions have lifetimes $\leqslant$10 μs, while the M + Na ions are considerably more stable. Similar behavior has been observed in many of the compounds we have studied.

The observation of the disintegration products at the same position as the parent ion is a particular property of a time-of-flight mass spectrometer. After such a break-up, each fragment retains the velocity of its parent ion plus or minus a small contribution due to the disintegration. The fragment therefore appears at the approximate position of the parent ion in the time-of-flight spectrum, but the peak is broadened because of the energy gained by the fragment in the break-up. Part, at least, of the observed broadening is caused by this effect.

Further examples of mass spectra obtained with this instrument, as well as comparisons with spectra excited by fission fragments, are presented elsewhere [19,20].

ACKNOWLEDGEMENTS

We are particularly indebted to Drs. D.F. Torgerson and R.D. Barber for helpful advice, and to Werner Ens for assistance in taking the data. We are also grateful to Dr. R.D. Macfarlane and to Dr. John Westmore for informative discussion. Loans of equipment from the Manitoba Cyclotron Laboratory, from Dr. R.D. Barber and from Dr. G. Tabisz are thankfully acknowledged.

This work was supported by grants from the University of Manitoba Research Board, and from the Natural Sciences and Engineering Research Council, Canada.

REFERENCES

1 G.D. Daves, Jr., Acc. Chem. Res., 12 (1979) 359.
2 R.D. Macfarlane and D.F. Torgerson, Science, 191 (1976) 920.
3 R.D. Macfarlane and D.F. Torgerson, Int. J. Mass Spectrom. Ion Phys., 21 (1976) 81.
4 A. Benninghoven and W. Sichtermann, Anal. Chem., 50 (1978) 1180.
5 P. Dück, W. Treu, W. Galster, H. Fröhlich and H. Voit, Nucl. Instrum. Methods, 168 (1980) 601.

6 R.D. Macfarlane, in George R. Waller and Otis C. Dermer (Eds.), Biochemical Applications of Mass Spectrometry, First Supplementary Volume, Wiley, New York, 1980, Ch. 38, pp. 1209—1217.
7 R.J. Day, S.E. Ungar and R.G. Cooks, Anal. Chem., 52 (1980) 557A; H. Grade and R.G. Cooks, J. Am. Chem. Soc., 100 (1978) 5615.
8 A. Eicke, W. Sichtermann and A. Benninghoven, Org. Mass Spectrom., 15 (1980) 289.
9 M. Barber, J.C. Vickerman and J. Wolstenholme, J. Chem. Soc., Faraday Trans. 1, 76 (1980) 549.
10 C.J. McNeal, R.D. Macfarlane and E.L. Thurston, Anal. Chem., 51 (1979) 2036.
11 J.P. Blewett and E.J. Jones, Phys. Rev., 50 (1936) 464.
12 S.K. Allison and M. Tamegai, Rev. Sci. Instrum., 32 (1961) 1090.
13 M.E. Haine and P.A. Einstein, Br. J. Appl. Phys., 3 (1952) 40.
14 M.E. Haine, P.A. Einstein and P.H. Borcherds, Br. J. Appl. Phys., 9 (1958) 482.
15 G. Liebmann, Proc. Phys. Soc. (London), B62 (1949) 213.
16 T.K. Fowler and W.M. Good, Nucl. Instrum. Methods, 7 (1962) 245.
17 R.F. Bonner, D.V. Bowen, B.T. Chait, A.B. Lipton and F.H. Field, Anal. Chem., 52 (1980) 1923.
18 N. Fürstenau, W. Knipperberg, F.R. Krueger, G. Weiss and K. Wien, Z. Naturforsch., 32a (1977) 711; N. Fürstenau, Z. Naturforsch., 33a (1978) 563.
19 K.G. Standing, W. Ens, B.T. Chait and F.H. Field, in A. Benninghoven (Ed.), Proc. Int. Conf. on Ion Formation from Organic Solids, Münster, W. Germany, 6—8 October 1980, Springer, Heidelberg, 1981, in press.
20 W. Ens, K.G. Standing, B.T. Chait and F.H. Field, Anal. Chem., 53 (1981) 1241.